

# Search for low mass dark gauge bosons at KLOE

**Enrico Graziani**

*on behalf of the KLOE/KLOE2 Collaboration*<sup>1</sup>

INFN sezione di Roma Tre, Roma, Italy

E-mail: [enrico.graziani@roma3.infn.it](mailto:enrico.graziani@roma3.infn.it)

**Abstract.** The existence of a light dark force mediator has been tested with the KLOE detector at DAΦNE. This particle, the so called dark photon  $U$ , has been searched for in three different processes and four different final states: a)  $\Phi \rightarrow \eta U$ , with  $U \rightarrow e^+e^-$ ,  $\eta \rightarrow \pi^+\pi^-\pi^0$  and  $\eta \rightarrow \pi^0\pi^0\pi^0$ ; b)  $e^+e^- \rightarrow U\gamma$  with  $U \rightarrow \mu^+\mu^-$ ; c)  $e^+e^- \rightarrow Uh'$  (dark Higgsstrahlung),  $U \rightarrow \mu^+\mu^-$ , where  $h'$  is a Higgs-like particle responsible for the breaking of the hidden symmetry.

We did not find any evidence of the processes above and set upper limits on the parameters of the model, for different  $M_U$  (and  $M_{h'}$ ) mass ranges, depending on the considered final state.

## 1. Introduction

In recent years, several unexpected astrophysical observations have failed to find a common interpretation in terms of standard astrophysical or particle physics sources. A non exhaustive list of these observations include the 511 keV gamma-ray signal from the galactic center observed by the INTEGRAL satellite [1], the excess in cosmic ray positrons reported by PAMELA [2], the total electron and positron flux measured by ATIC [3], Fermi [4], and HESS [5, 6], the annual modulation of the DAMA/LIBRA signal [7, 8] and the low energy spectrum of nuclear recoil candidate events observed by CoGeNT [9].

Although there are alternative explanations for some of these anomalies, they could be all explained with the existence of a dark matter weakly interacting massive particle, WIMP, belonging to a secluded gauge sector under which the Standard Model (SM) particles are uncharged [10, 11, 12, 13, 14]. An abelian gauge field, the  $U$  boson with mass near the GeV scale, couples the secluded sector to the SM through its kinetic mixing with the SM hypercharge gauge field. The kinetic mixing parameter  $\epsilon$  is expected to be of the order  $10^{-4} - 10^{-2}$  [11, 12, 13, 14, 15], so that observable effects can be induced in  $O(\text{GeV})$ -energy  $e^+e^-$  colliders [15, 16, 17] and fixed target experiments [18, 19, 20].

<sup>1</sup> D. Babusci, D. Badoni, I. Balwierz-Pytko, G. Bencivenni, C. Bini, C. Bloise, F. Bossi, P. Branchini, A. Budano, L. Caldeira Balkestahl, G. Capon, F. Ceradini, P. Ciambione, F. Curciarello, E. Czerwiński, E. Dané, V. De Leo, E. De Lucia, G. De Robertis, A. De Santis, P. De Simone, A. Di Domenico, C. Di Donato, R. Di Salvo, D. Domenici, O. Erriquez, G. Fanizzi, A. Fantini, G. Felici, S. Fiore, P. Franzini, P. Gauzzi, G. Giardina, S. Giovannella, F. Gonnella, E. Graziani, F. Happacher, L. Heijkskjöld, B. Höistad, L. Iafolla, E. Iarocci, M. Jacewicz, T. Johansson, K. Kacprzak, W. Kluge, A. Kupsc, J. Lee-Franzini, F. Loddo, P. Lukin, G. Mandaglio, M. Martemianov, M. Martini, M. Mascolo, R. Messi, S. Miscetti, G. Morello, D. Moricciani, P. Moskal, S. Muller, F. Nguyen, A. Passeri, V. Patera, I. Prado Longhi, A. Ranieri, C. F. Redmer, P. Santangelo, I. Sarra, M. Schioppa, B. Sciascia, M. Silarski, C. Taccini, L. Tortora, G. Venanzoni, R. Versaci, W. Wiślicki, M. Wolke, J. Zdebik



The  $U$  boson can be produced at  $e^+e^-$  colliders via different processes:  $V \rightarrow PU$  decays, where  $V$  and  $P$  are vector and pseudoscalar mesons, respectively ( $\Phi$  and  $\eta$  in the case of KLOE),  $e^+e^- \rightarrow U\gamma$  and  $e^+e^- \rightarrow Uh'$  (dark Higgsstrahlung), where  $h'$  is a Higgs-like particle responsible for the breaking of the hidden symmetry.

KLOE is in a very good position to probe the existence of a dark light sector at the GeV scale because a) it operates on DAΦNE exactly at the GeV scale; b) most of the interesting dark process cross sections scale as  $1/s$ , i.e. a factor  $\sim 100$  with respect to the B factories; c) it is a unique place to study the rare  $\Phi$  meson decays.

## 2. The KLOE detector

The KLOE experiment operated from 2000 to 2006 at DAΦNE, the Frascati  $\Phi$  factory. DAΦNE is an  $e^+e^-$  collider running mainly at a center-of-mass energy of  $\sim 1019$  MeV, the mass of the  $\Phi$  meson. Equal energy positron and electron beams collide at an angle of  $\sim 25$  mrad, producing  $\Phi$  mesons nearly at rest. The detector consists of a large cylindrical Drift Chamber (DC) [21], which provides a momentum resolution  $\sigma_{\perp}/p_{\perp} \approx 0.4$ , surrounded by a lead-scintillating fiber electromagnetic calorimeter (EMC) [21], with energy and time resolutions  $\sigma_E/E = 5.7\%/\sqrt{E(\text{GeV})}$  and  $\sigma_t = 57 \text{ ps}/\sqrt{E(\text{GeV})} \oplus 100 \text{ ps}$ , respectively. A superconducting coil around the EMC provides a 0.52 T field.

## 3. $U$ boson search in $\Phi \rightarrow \eta U$ decay

We study the process  $\Phi \rightarrow \eta U$  using a sample of  $\Phi$  mesons produced resonantly at the DAΦNE collider. The  $U$  boson can be observed by its decay into a lepton pair, while the  $\eta$  can be tagged by one of its main decays. The best  $U$  decay channel in KLOE to look for is  $U \rightarrow e^+e^-$ , since a wider range of  $U$  boson masses can be tested and  $e^{\pm}$  are easily identified using a time-of-flight (ToF) technique. As far as the  $\eta$  decays are concerned, we used both the three pion decay modes:  $\eta \rightarrow \pi^+\pi^-\pi^0$  and  $\eta \rightarrow \pi^0\pi^0\pi^0$ . An irreducible background due to the Dalitz decay of the  $\Phi$  meson,  $\Phi \rightarrow \eta e^+e^-$ , is present. This is expected to have a cross section of the order of  $\sim 0.7$  nb, to be compared with the signal cross section which, for  $\epsilon = 10^{-3}$ , is predicted to be  $\sim 40$  fb. Despite the small ratio between the  $\Phi \rightarrow \eta U$  and the overall  $\Phi \rightarrow \eta e^+e^-$ , their different dilepton invariant mass distribution allows to test the parameter  $\epsilon$  down to  $10^{-3}$ , with the KLOE data set of  $1.5 \text{ fb}^{-1}$  (corresponding to  $\approx 5 \times 10^9 \Phi$ ). The Monte Carlo simulation of the irreducible Dalitz  $\Phi$  decay background has been produced with a Vector Meson Dominance model [23]. Different preselection cuts are chosen depending on the selected  $\eta$  decay channel. For  $\eta \rightarrow \pi^+\pi^-\pi^0$  decay:

- two positive and two negative tracks with points of closest approach to the beam line inside a  $4 \times 20$  cm cylinder around the interaction point;
- two prompt photon candidates, i.e. two energy clusters with  $E > 7$  MeV not associated to any track, in an angular acceptance  $|\cos\theta_{\gamma}| < 0.92$  and in the expected time window for a photon  $|T_{\gamma} - R_{\gamma}/c| < \min(5\sigma_T, 2ns)$ ;
- best  $\pi^+\pi^-\gamma\gamma$  match to the  $\eta$  mass in the pion hypothesis (the other two tracks are then assigned to  $e^{\pm}$ );
- loose cuts of about  $\pm 4\sigma$ 's on  $\eta$  and  $\pi^0$  invariant masses ( $495 < M_{\pi^+\pi^-\gamma\gamma} < 600$  MeV,  $70 < M_{\gamma\gamma} < 200$  MeV);
- a cut on the recoil mass to the  $e^+e^-\pi^+\pi^-$  system, which is expected to be equal to the  $\pi^0$  mass for signal events:  $100 < M_{recoil}(ee\pi\pi) < 160$  MeV.

For  $\eta \rightarrow \pi^0\pi^0\pi^0$  decay:

- two opposite charge tracks with points of closest approach to the beam line inside a  $4 \times 20$  cm cylinder around the interaction point;

- six prompt photon candidates, i.e. energy clusters with  $E > 7$  MeV not associated to any track, in an angular acceptance  $|\cos\theta_\gamma| < 0.92$  and in the expected time window for a photon  $|T_\gamma - R_\gamma/c| < \min(3\sigma_T, 2ns)$ ;
- a loose cut on the six photon invariant mass  $400 < M_{6\gamma} < 700$  MeV).

After these selections, a clear peak corresponding to the  $\eta$  mass is observed in the distribution of the recoil mass against the  $e^+e^-$  pair, in both samples. Residual contaminations due to  $\Phi \rightarrow \eta\gamma$  events with photon conversion on beam pipe or drift chamber walls are strongly rejected by tracing back the tracks of the  $e^\pm$  candidates, reconstructing their invariant mass and their distance at the conversion surfaces and cutting on these variables. Further selections, aimed at applying some particle identification (PID) requirement to electrons, are implemented. This is achieved by exploiting the timing capabilities of the calorimeter. When an energy cluster is associated to a track, the time of flight (ToF) to the calorimeter is evaluated both using the track trajectory ( $T_{track} = L_{track}/\beta c$ ) and the calorimeter timing ( $T_{cluster}$ ). The  $\Delta T = T_{track} - T_{cluster}$  variable is then evaluated in the electron hypothesis ( $\Delta T_e$ ). In order to be fully efficient on the signal, events with either an  $e^+$  or an  $e^-$  candidate inside a  $3\sigma$  window around  $\Delta T_e = 0$  are retained for further analysis.

At the end of the analysis chains, the background contaminations were evaluated to be 3% and 2% for the  $\eta \rightarrow \pi^+\pi^-\pi^0$  and  $\eta \rightarrow \pi^0\pi^0\pi^0$  channels respectively. The analysis signal efficiencies ranged between 10% and 20%, depending on  $M_{ee}$ , for the  $\eta \rightarrow \pi^+\pi^-\pi^0$  sample, and between 15% and 30% for the  $\eta \rightarrow \pi^0\pi^0\pi^0$  sample.

The upper limit on the  $U$  boson production in the  $\Phi \rightarrow \eta U$  process is obtained by combining the two  $\eta$  decay channels. The resolution of the  $e^+e^-$  invariant mass has been found to be below 2 MeV over the full mass range. The determination of the limit is done by varying the  $M_U$  mass with 1 MeV step, in the range between 5 and 470 MeV. For each channel, the irreducible background is extracted directly from data after applying a bin by bin subtraction of the non-irreducible backgrounds and correcting for the analysis efficiency. The  $M_{ee}$  distribution is then fitted with a parametrized function (representing the transition form factor) excluding the bins used in the upper limit evaluation. The exclusion limit on the number of events for the  $\Phi \rightarrow \eta U$  signal as a function of  $M_U$  is obtained with the CLS technique [24], using the  $M_{ee}$  spectra before background subtraction. The limit is extracted both for each  $\eta$  decay channel and in a combined way. In fig. 1 top, the upper limit at 90% CL on the number of events for the decay chain  $\Phi \rightarrow \eta U$ ,  $U \rightarrow e^+e^-$ , is shown for both  $\eta \rightarrow \pi^+\pi^-\pi^0$  and  $\eta \rightarrow \pi^0\pi^0\pi^0$ , separately evaluated.

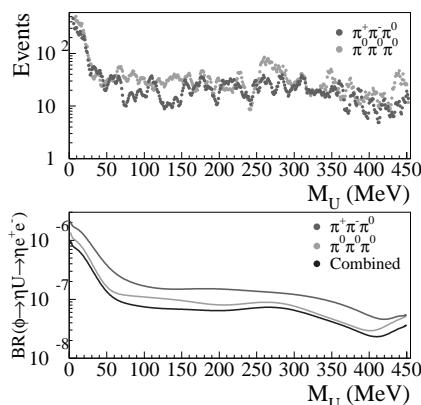


**Figure 1.** Top: upper limit at 90% CL on the number of events for the decay chain  $\eta \rightarrow \pi^0\pi^0\pi^0$  and  $\eta \rightarrow \pi^+\pi^-\pi^0$ . Bottom: smoothed upper limit at 90% CL on  $BR(\Phi \rightarrow \eta U) \times BR(U \rightarrow e^+e^-)$  obtained separately for the two  $\eta$  decay channels and from the combined analysis.

In fig.1 bottom, the smoothed upper limit on the branching fraction for the process  $\Phi \rightarrow \eta U$ ,  $U \rightarrow e^+e^-$ , obtained for the combined method is compared with evaluations from each of

the two decay channels. In the combined result, the upper limit on the product  $BR(\Phi \rightarrow \eta U) \times BR(U \rightarrow e^+e^-)$  varies from  $10^{-6}$  at small  $M_U$  to  $\sim 3 \times 10^{-8}$  at 450 MeV. The exclusion plot in the  $\alpha'/\alpha = \epsilon^2 vs M_U$  plane, where  $\alpha'$  is the coupling of the  $U$  bosons to electrons and  $\alpha$  is the fine structure constant, has been finally derived for two different transition form factor hypotheses. In fig. 2 the smoothed exclusion plot at 90% CL on  $\alpha'/\alpha$  is compared with existing limits in the same region of interest. This result reduces the region of the  $U$  boson parameters that could explain the observed discrepancy between the Standard Model prediction of the muon anomalous magnetic moment,  $a_\mu$ , ruling out masses in the range 60-435 MeV

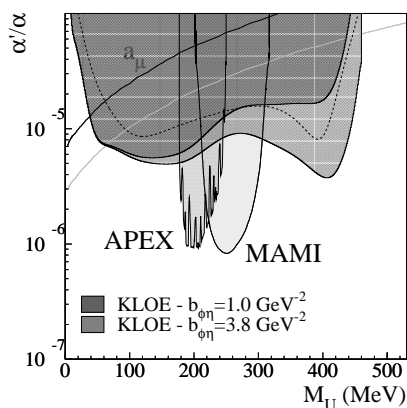


**Figure 2.** Exclusion plot at 90% CL for the parameter  $\alpha'/\alpha = \epsilon^2$ , compared with existing limits from the muon anomalous magnetic moment and from MAMI/A1 and APEX experiments. The gray line represents the expected values of the  $U$  boson parameters needed to explain the observed discrepancy between measured and calculated  $a_\mu$  values. The dotted line is the previous KLOE result obtained with the  $\eta \rightarrow \pi^+\pi^-\pi^0$  channel only.

#### 4. $U$ boson search in $e^+ + e^- \rightarrow \mu^+\mu^-\gamma$

The expected signal here is the appearance of a Breit-Wigner peak in the invariant mass distribution of the  $\mu^+\mu^-$  pair. The analysis described in the following is based on the KLOE pion form factor measurement[25]. The data sample consists of  $239.29 pb^{-1}$  of KLOE data taken during the year 2002. The event selection requires:

- two charged tracks with  $50^\circ < \theta_\mu < 130^\circ$ ;
- one photon within a cone of  $\theta_\gamma < 15^\circ$  ( $\theta_\gamma > 165^\circ$ ) around the beamline.

The photon is not detected and its direction is reconstructed from event kinematics:  $\vec{p}_\gamma \simeq \vec{p}_{miss} \equiv -\vec{p}_{\mu\mu} = -(\vec{p}_{\mu^+} + \vec{p}_{\mu^-})$ . This selection greatly reduces the contamination from the resonant process  $e^+e^- \rightarrow \Phi \rightarrow \pi^+\pi^-\pi^0$ , where the  $\pi^0$  mimics the missing momentum of the photon(s), and from the final state radiation processes:  $e^+e^- \rightarrow \pi^+\pi^-\gamma_{FSR}$  and  $e^+e^- \rightarrow \mu^+\mu^-\gamma_{FSR}$ . The  $M_{trk}$  variable is computed from energy and momentum conservation, assuming the presence of an unobserved photon and in the assumption of equal mass charged particles.

Background contributions coming from  $e^+e^- \rightarrow \pi^+\pi^-\gamma(\gamma)$ ,  $e^+e^- \rightarrow \Phi \rightarrow \pi^+\pi^-\pi^0$  and  $e^+e^- \rightarrow e^+e^-\gamma(\gamma)$  were separated applying kinematical cuts in the  $M_{trk} - M_{\pi\pi}^2$  plane. A particle identification estimator (PID), based on a pseudo-likelihood function using the time-of-flight and calorimeter information, was used to suppress radiative Bhabha events. Finally pions and muons are separated by cuts on the trackmass variable  $M_{trk}$ :

- muons:  $80 < M_{trk} < 115$  MeV,
- pions:  $M_{trk} > 130$  MeV.

The contributions of the three background channels surviving the  $\mu^+\mu^-\gamma$  selections are obtained by fitting in slices of  $M_{\mu\mu}^2$  the  $M_{trk}$  distributions for data as a superposition of signal and

background distributions. The  $M_{trk}$  distributions for  $\mu^+\mu^-\gamma$ ,  $\pi^+\pi^-\gamma$ ,  $\pi^+\pi^-\pi^0$  were extracted by Monte Carlo calculation. A further separation between pions and muons was performed by a cut on the  $\sigma_{Mtrk}$  variable, which parametrizes the quality of the fit of the tracks. Once the Data/MC corrections have been applied, the  $\mu^+\mu^-\gamma$  cross section was extracted by subtracting the residual background to the observed spectra and dividing it by efficiency and luminosity. The absolute cross section is in good agreement with the PHOKHARA prediction[26], as shown in Fig. 3.

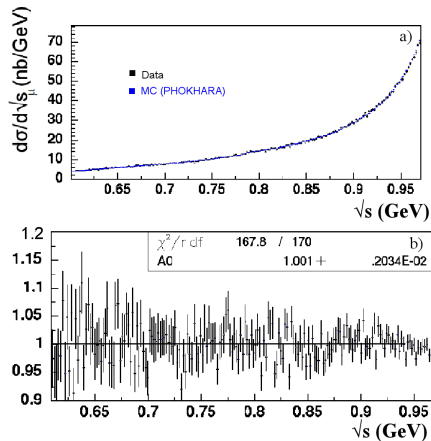


**Figure 3.** *a) Comparison of data (black points) and MC (blue points) of  $\mu^+\mu^-\gamma$  absolute cross section b) ratio of data and MC PHOKHARA prediction*

No signal is observed (fig. 3 top). To extract the upper limit on  $\varepsilon^2$  the CLS technique[24] was used, with the observed spectrum and the PHOKHARA spectrum as input and background to the procedure. A systematic error of  $\sim 2\%$  on background was also applied. The 90% CL upper limits in terms of number of events were then extracted, in the energy range between 600 and 1000 MeV. They were later converted in terms of the mixing parameter  $\varepsilon^2$  by using the analysis selection efficiency, the integrated luminosity, the  $e^+e^- \rightarrow \mu^+\mu^-$  differential cross section and the predicted  $U$  boson production cross section. In Fig.4 the kinetic mixing parameter  $\varepsilon^2$  in the 600-1000 MeV range and the other existing limits are presented. The blue area is the present measurement, with 90% CL exclusion limits between  $2.6 \times 10^{-6}$  and  $3.5 \times 10^{-7}$ , and with the clearly visible reduction of sensitivity in the  $\rho$  meson region. The red and dark green areas represent the Mami results[27], and the Apex measurements[28] respectively. The black line represents the  $\varepsilon^2$  values consistent with a  $U$  boson contribution to the muon magnetic moment anomaly  $a_\mu$ .

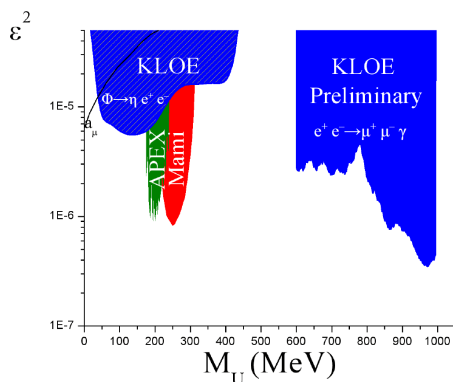


**Figure 4.** *Exclusion Plot on  $\varepsilon^2$  compared with the existing limits in the 0 – 1000 MeV range*

### 5. $U$ boson search through the dark Higgsstrahlung process

The process  $e^+e^- \rightarrow Uh'$  is one of the most interesting reactions to study at an  $e^+e^-$  collider because, differently from the other final states above, is suppressed by a single factor of  $\epsilon$ . There are two very different scenarios depending on the masses of the dark photon and of the dark Higgs boson. For Higgs boson mass  $M_{h'}$  larger than two dark photon masses  $M_U$ , the dark Higgs boson would decay dominantly and promptly to a  $U$  boson pair, thus giving rise to a six charged particle final state (this case was recently investigated by the BaBar experiment [29]); while Higgs bosons lighter than the dark photon would have, in most of the parameter space region, such a large lifetime to escape undetected, showing up as a missing energy signature. Here we study only the so called “invisible” dark Higgs scenario, thus confining the search to the case  $M_{h'} < M_U$ .

The lifetime of the dark Higgs boson depends on the kinetic mixing parameter  $\epsilon$ , the boson masses  $M_{h'}$  and  $M_U$  and the dark coupling constant  $\alpha_D$ . For masses of the order of 100 MeV and  $\alpha_D = \alpha$  the dark Higgs boson lifetime would be  $\sim 5\mu\text{s}$  for  $\epsilon \sim 10^{-3}$ , corresponding, for KLOE energies, to a decay length of  $\sim 100$  m. The dark Higgs boson would be invisible up to  $\epsilon \sim 10^{-2} \div 10^{-1}$ , depending on the  $h'$  mass.

We limit our search to the decay of the  $U$  boson in a muon pair: our final state signature is then a couple of opposite charge muons plus missing energy. The measurement is thus performed in the range  $2M_\mu < M_U < 1000$  MeV with the constraint  $M_{h'} < M_U$ .

The production cross section of the dark Higgsstrahlung process is proportional to the product  $\alpha_D \times \epsilon^2$  and depends on the boson masses [16]. Values as high as hundreds of fb are reachable in the hypothesis  $\epsilon = 10^{-3}$  and  $\alpha_D = \alpha$ .

The analysis of the process has been performed on a data sample of  $1.65 \text{ fb}^{-1}$  collected during the 2004-2005 KLOE data taking campaign at a center of mass energy of  $\sim 1019$  MeV, corresponding to the mass of the  $\Phi$  meson (on peak sample), and on a data sample of  $0.2 \text{ fb}^{-1}$  at a center of mass energy of  $\sim 1000$  MeV (off peak sample), well below the  $\Phi$  resonance.

The mass resolution was found to be between 0.5 and 2 MeV for  $M_U$  (invariant mass of the muon pair) and between 3 and 17 MeV for  $M_{h'}$  (missing mass). The signature of the process would thus be the appearance of a sharp peak in the bidimensional distribution  $M_{\mu\mu} - M_{\text{miss}}$ . Contrarily to most of the dominant QED background processes, the signal is predicted to show a large angle production in  $\theta$ , with two dominant terms proportional to  $\sin\theta$  and  $\sin^3\theta$  [16].

As a first step of the analysis, a preselection was performed by requiring:

- events with only two opposite charge tracks, with a reconstructed vertex inside a  $4 \times 30$  cm cylinder around the interaction point;
- each track must have an associated EMC cluster;
- the visible momentum direction has to be in the barrel:  $|\cos\theta| < 0.75$ ;
- the momenta of the two tracks must be individually below 460 MeV;
- the modulus of the missing momentum must exceed 40 MeV.

After this selections (mostly aimed at rejecting QED backgrounds), the hermeticity and tightness of the electromagnetic calorimeter was used as a veto to avoid the presence of photons in the event. It was required to have no unassociated energy deposition with  $E > 15$  MeV on EMC.

The event selection then proceeded by applying particle identification (PID) algorithms to the two charged tracks. These were almost entirely based on the excellent energy and time resolution of the EMC, through a set of neural networks, organised for different values of track momentum and polar angle. The PID performances, checked on selected data samples of  $e^+e^- \rightarrow e^+e^-$ ,  $e^+e^- \rightarrow \mu^+\mu^-$ ,  $e^+e^- \rightarrow \pi^+\pi^-$  were found to be excellent: the fraction of  $e^+e^- \rightarrow \mu^+\mu^-$  events, in which both tracks were required to be identified as muons, was measured to be 85%, while the fraction of residual  $e^+e^- \rightarrow e^+e^-$  events was  $10^{-4}$  and the fraction of doubly tagged  $e^+e^- \rightarrow \pi^+\pi^-$  was  $\sim 50\%$  (muon and pion induced showers look very similar at KLOE energies).

After the missing energy and the PID selections, a huge background from  $\Phi \rightarrow K^+K^-$ ,  $K^\pm \rightarrow \mu^\pm\nu$  events survives in the on peak sample. This corresponds to the fraction of doubly early leptonically decaying charged kaons in the IP region. Cuts on the radial and z projections of the distance between the reconstructed vertex and the IP and on the  $\chi^2$  of the fit allowed to reduce by a factor  $\sim 35$  the  $\Phi \rightarrow K^+K^-$ ,  $K^\pm \rightarrow \mu^\pm\nu$  background.

Events surviving all the described selections were organized in bidimensional histograms with the muon pair mass  $M_{\mu\mu}$  and the event missing mass  $M_{miss}$  on the two axes. The binning was chosen such as to keep most of the signal in one bin only. In  $M_{\mu\mu}$  a 5 MeV bin width was enough over all the plane; while for  $M_{miss}$  a variable binning of 15, 30 and 50 MeV widths was chosen. The selection efficiency, estimated from Monte Carlo, was found to be between 15% and 25%, depending on the masses, with most frequent values  $\sim 20\%$ . A total  $\pm 10\%$  systematic uncertainty on the selection efficiency was conservatively estimated.

Results are shown in fig. 5 for the on peak and off peak samples. In the left plot of fig. 5 (on peak sample) several sources of backgrounds are easily distinguishable:  $\Phi \rightarrow K^+K^-$ ,  $K^\pm \rightarrow \mu^\pm\nu$  (triangular region at the left of the populated part of the distribution),  $\Phi \rightarrow \pi^+\pi^-\pi^0$  (mostly horizontal band, corresponding to events in which both photons from  $\pi^0$  decay are undetected), continuum backgrounds  $e^+e^- \rightarrow \mu^+\mu^-$  and  $e^+e^- \rightarrow \pi^+\pi^-$  (diagonal bands starting from the right-bottom part of the distribution),  $e^+e^- \rightarrow e^+e^-\mu^+\mu^-$  and  $e^+e^- \rightarrow e^+e^-\pi^+\pi^-$  (two photon events, top part of the distribution, for  $M_{miss} > 350\text{MeV}$ ). In the distribution in the right plot of fig. 5 (off peak sample) all the backgrounds from the  $\Phi$  decays are strongly suppressed.

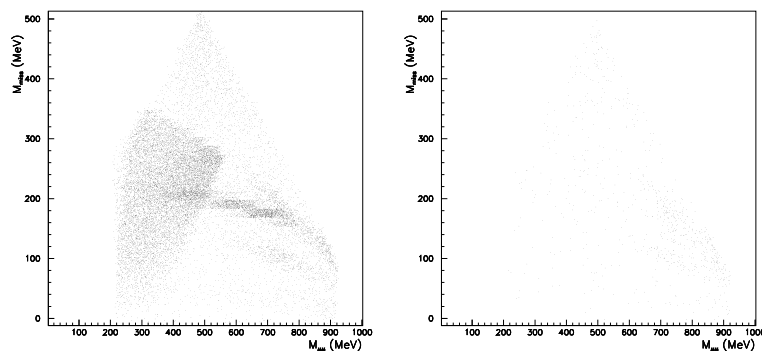


**Figure 5.** Results for on peak sample (left plot,  $1.65\text{ fb}^{-1}$  integrated luminosity) and off peak sample (right plot,  $0.2\text{ fb}^{-1}$  integrated luminosity).

The background was evaluated directly on the data, by counting populations in bins adjacent to the one in which the signal is looked for. No evidence of the dark Higgsstrahlung process was found (see fig. 5). Using uniform prior distributions, 90% confidence level Bayesian upper limits on the number of events were derived, separately for the on peak and off peak samples. These results were then converted in terms of the dark Higgsstrahlung production cross section parameters  $\alpha_D \times \epsilon^2$  by using the integrated luminosity information, the signal efficiency, the predicted dark Higgsstrahlung cross section and the branching fraction of the  $U$  boson decay into muon pairs as in reference [16]. The on peak and off peak limits were combined and projected in the  $M_{\mu\mu}$  and  $M_{miss}$  directions (slightly smoothed, just to make them more readable). They are shown in fig. 6. Values as low as  $10^{-9} \div 10^{-8}$  in  $\alpha_D \epsilon^2$  are excluded at 90% CL for a large range of the dark photon and dark Higgs masses.

These results are numerically comparable with those of Babar [29] and complement them as they refer to the same process in a different final state and in a different region of the phase space.

At KLOE2/DAΦNE2 the larger integrated luminosity and the presence of a high resolution Inner Tracker detector are expected to improve these results at least by a factor 2, thus allowing a study deep inside the  $\epsilon \approx 10^{-4}$  parameter space region.

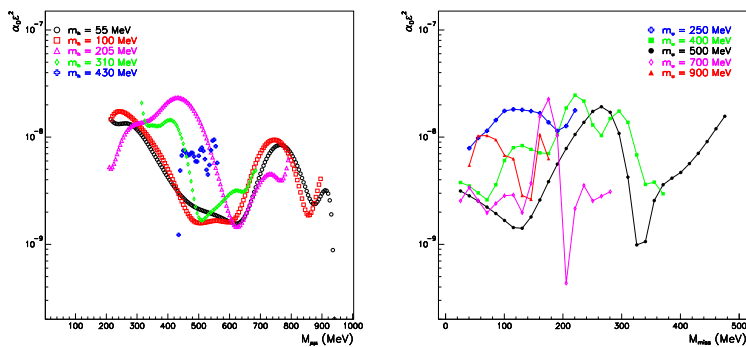


**Figure 6.** Combined 90% CL upper limits in  $\alpha_D \epsilon^2$  as a function of  $M_{\mu\mu}$  for different values of  $M_{h'}$  (left plot) and as a function of  $M_{miss}$  for different values of  $M_U$  (right plot).

## Conclusions

KLOE searched for a dark gauge  $U$  boson in three different processes and four different final states: a)  $\Phi \rightarrow \eta U$ , with  $U \rightarrow e^+e^-$ ,  $\eta \rightarrow \pi^+\pi^-\pi^0$  and  $\eta \rightarrow \pi^0\pi^0\pi^0$ ; b)  $e^+e^- \rightarrow U\gamma$  with  $U \rightarrow \mu^+\mu^-$ ; c)  $e^+e^- \rightarrow U h'$  (dark Higgsstrahlung),  $U \rightarrow \mu^+\mu^-$ . We found no evidence and set upper limits on the mixing parameter  $\epsilon^2$  with the Standard Model, as a function of the  $U$  mass, in the range  $10^{-5} \div 10^{-7}$ , depending on the process. The upgraded DAΦNE2 luminosity and the insertion of new detectors in KLOE2 are expected to improve these limits by a factor 2÷4.

## References

- [1] P.Jean *et al.* Astron. Astrophys., **407** (2003), p. L55
- [2] O. Adriani *et al.* Nature, **458** (2009), p. 607
- [3] J. Chang *et al.* Nature, **456** (2008), p. 362
- [4] A.A. Abdo *et al.* Phys. Rev. Lett., **102** (2009), p. 181101
- [5] F. Aharonian *et al.* Phys. Rev. Lett., **101** (2008), p. 261104
- [6] F. Aharonian *et al.* Astron. Astrophys., **508** (2009), p. 561
- [7] R. Bernabei *et al.* Int. J. Mod. Phys. D, **13** (2004), p. 2127
- [8] R. Bernabei *et al.* Eur. Phys. J. C, **56** (2008), p. 333
- [9] C.E. Aalseth *et al.* Phys. Rev. Lett., **107** (2011), p. 141301
- [10] M. Pospelov, A. Ritz, M.B. Voloshin Phys. Lett. B, **662** (2008), p. 53
- [11] N. Arkani-Hamed, D.P. Finkbeiner, T.R. Slatyer, N. Weiner Phys. Rev. D, **79** (2009), p. 015014
- [12] D.S.M. Alves, S.R. Behbahani, P. Schuster, J.G. Wacker Phys. Lett. B, **692** (2010), p. 323
- [13] M. Pospelov, A. Ritz Phys. Lett. B, **671** (2009), p. 391
- [14] N. Arkani-Hamed, N. Weiner JHEP, **0812** (2008), p. 104
- [15] R. Essig, P. Schuster, N. Toro Phys. Rev. D, **80** (2009), p. 015003
- [16] B. Batell, M. Pospelov, A. Ritz Phys. Rev. D, **79** (2009), p. 115008
- [17] M. Reece, L.T. Wang JHEP, **0907** (2009), p. 051
- [18] J.D. Bjorken, R. Essig, P. Schuster, N. Toro Phys. Rev. D, **80** (2009), p. 075018
- [19] B. Batell, M. Pospelov, A. Ritz Phys. Rev. D, **80** (2009), p. 095024
- [20] R. Essig, P. Schuster, N. Toro, B. Wojtsekhowski JHEP, **1102** (2011), p. 009
- [21] M. Adinolfi *et al.* Nucl. Instr. Meth. A, **488** (2002), p. 51
- [22] M. Adinolfi *et al.* Nucl. Instr. Meth. A, **482** (2002), p. 364
- [23] L.G. Landsberg, Phys. Rep. **128** (1985), p. 301
- [24] G. C. Feldman, R. D. Cousins, Physical Rev. D **57**, 3873 (1998)
- [25] D. Babusci *et al.*, arXiv:1212.4524 [KLOE/KLOE2 Collaboration]
- [26] H. Czyż *et al.*, Eur. Phys. J. C **39** 411 (2005)
- [27] M. Merkel *et al.*, Phys. Rev. Lett. **106**, 251802 (2011)
- [28] S. Abrahamyan *et al.*, Phys. Rev. Lett. **107**, 191804 (2011)
- [29] J.P. Lees *et al.* (BaBar Collab.) Phys. Rev. Lett. **108** (2012) 211801